

Pseudorapidity Distributions of Charged Particles Produced in $\bar{p}p$ Interactions at $\sqrt{s} = 630$ and 1800 GeV *

F. Abe¹⁶, D. Amidei³, G. Apollinari¹¹, G. Ascoli⁷, M. Atac⁴, P. Auchincloss¹⁴, A.R. Baden⁶, A. Barbaro-Galtieri⁹, V.E. Barnes¹², F. Bedeschi¹¹, S. Belforte¹¹, G. Belletini¹¹, J. Bellinger¹⁷, J. Bensinger², A. Beretvas¹⁴, P. Berge⁴, S. Bertolucci⁵, S. Bhadra⁷, M. Binkley⁴, R. Blair¹, C. Blocker², J. Bofill⁴, A.W. Booth⁴, G. Brandenburg⁶, D. Brown⁶, A. Byon¹², K.L. Byrum¹⁷, M. Campbell³, R. Carey⁶, W. Carithers⁹, D. Carlsmith¹⁷, J.T. Carroll⁴, R. Cashmore⁴, F. Cervelli¹¹, K. Chadwick^{4,12}, T. Chapin¹³, G. Chiarelli¹¹, W. Chinowsky⁹, S. Cihangir¹⁵, D. Cline¹⁷, D. Connor¹⁰, M. Contreras², J. Cooper⁴, M. Cordelli⁵, M. Curatolo⁵, C. Day⁴, R. DeFabbro¹¹, M. Dell'Orso¹¹, L. DeMortier², T. Devlin¹⁴, D. DiBitonto¹⁵, R. Diebold¹, F. Dittus⁴, A. DiVirgilio¹¹, J. Elias⁴, R. Ely⁹, S. Errede⁷, B. Esposito⁵, B. Flaughner¹⁴, E. Focardi¹¹, G.W. Foster⁴, M. Franklin^{6,7}, J. Freeman⁴, H. Frisch³, Y. Fukui⁸, A.F. Garfinkel¹², P. Giannetti¹¹, N. Giokaris¹³, P. Giromini⁵, L. Gladney¹⁰, M. Gold⁹, K. Goulios¹³, C. Grosso-Pilcher³, C. Haber⁹, S.R. Hahn¹⁰, R. Handler¹⁷, R.M. Harris⁹, J. Hauser³, T. Hessing¹⁵, R. Hollebeek¹⁰, P. Hu¹⁴, B. Hubbard⁹, P. Hurst⁷, J. Huth⁴, H. Jensen⁴, R.P. Johnson⁴, U. Joshi¹⁴, R.W. Kadel⁴, T. Kamon¹⁵, S. Kanda¹⁶, D.A. Kardelis⁷, I. Karliner⁷, E. Kearns⁶, R. Kephart⁴, P. Kesten², H. Keutelian⁷, S. Kim¹⁶, L. Kirsch², K. Kondo¹⁶, U. Kruse⁷, S.E. Kuhlmann¹², A.T. Laasanen¹², W. Li¹, T. Liss³, N. Lockyer¹⁰, F. Marchetto¹⁵, R. Markeloff¹⁷, L.A. Markosky¹⁷, P. McIntyre¹⁵, A. Menzione¹¹, T. Meyer¹⁵, S. Mikamo⁸, M. Miller¹⁰, T. Mimashi¹⁶, S. Miscetti⁵, M. Mishina⁸, S. Miyashita¹⁶, N. Mondal¹⁷, S. Mori¹⁶, Y. Morita¹⁶, A. Mukherjee⁴, C. Newman-Holmes⁴, L. Nodulman¹, R. Paoletti¹¹, A. Para⁴, J. Patrick⁴, T.J. Phillips⁶, H. Piekarz², R. Plunkett¹³, L. Pondrom¹⁷, J. Proudfoot¹, G. Punzi¹¹, D. Quarrie⁴, K. Ragan¹⁰, G. Redlinger³, J. Rhoades¹⁷, F. Rimondi⁴, L. Ristori¹¹, T. Rohaly¹⁰, A. Roodman³, A. Sansoni⁵, R. Sard⁷, V. Scarpine⁷, P. Schlabach⁷, E.E. Schmidt⁴, P. Schoessow¹, M.H. Schub¹², R. Schwitters⁶, A. Scribano¹¹, S. Segler⁴, M. Sekiguchi¹⁶, P. Sestini¹¹, M. Shapiro⁶, M. Sheaff¹⁷, M. Shibata¹⁶, M. Shochet³, J. Siegrist⁹, P. Sinervo¹⁰, J. Skarha¹⁷, D.A. Smith⁷, F.D. Snider³, R. St.Denis⁶, A. Stefanini¹¹, Y. Takaiwa¹⁶, K. Takikawa¹⁶, S. Tarem², D. Theriot⁴, A. Tollestrup⁴, G. Tonelli¹¹, Y. Tsay³, F. Ukegawa¹⁶, D. Underwood¹, R. Vidal⁴, R.G. Wagner¹, R.L. Wagner⁴, J. Walsh¹⁰, T. Watts¹⁴, R. Webb¹⁵, T. Westhusing⁷, S. White¹³, A. Wicklund¹, H.H. Williams¹⁰, T. Yamanouchi⁴, A. Yamashita¹⁶, K. Yasuoka¹⁶, G.P. Yeh⁴, J. Yoh⁴, F. Zetti¹¹

¹Argonne National Laboratory, Argonne, Illinois 60439 • ²Brandeis University, Waltham, Massachusetts 02254 •

³University of Chicago, Chicago, Illinois 60637 • ⁴Fermi National Accelerator Laboratory,

P.O. Box 500, Batavia, Illinois 60510 • ⁵Laboratori Nazionali di Frascati, Istituto Nazionale di Fisica Nucleare, I-00044, Frascati, Italy • ⁶Harvard University, Cambridge, Massachusetts 02138 • ⁷University of Illinois, Urbana, Illinois 61801 •

⁸National Laboratory for High Energy Physics (KEK), Tsukuba, Ibaraki 305, Japan • ⁹Lawrence Berkeley Laboratory, Berkeley, California 94720 • ¹⁰University of Pennsylvania, Philadelphia, Pennsylvania 19104 •

¹¹INFN, University and Scuola Normale Superiore of Pisa, Pisa, Italy • ¹²Purdue University, West Lafayette, Indiana 47907 •

¹³Rockefeller University, New York, New York 10021 • ¹⁴Rutgers University, Piscataway, New Jersey 08854 •

¹⁵Texas A&M University, College Station, Texas 77843 • ¹⁶University of Tsukuba, Tsukuba, Ibaraki 305, Japan •

¹⁷University of Wisconsin, Madison, Wisconsin 53706

September 1989

*Submitted to Phys. Rev. Lett.



Operated by Universities Research Association, Inc., under contract with the United States Department of Energy

Pseudorapidity Distributions of Charged Particles Produced in $\bar{p}p$ Interactions

at $\sqrt{s} = 630$ and 1800 GeV

F. Abe,⁽¹⁶⁾ D. Amidei,⁽³⁾ G. Apollinari,⁽¹¹⁾ G. Ascoli,⁽⁷⁾ M. Atac,⁽⁴⁾ P. Auchincloss,⁽¹⁴⁾ A. R. Baden,⁽⁶⁾
A. Barbaro-Galtieri,⁽⁹⁾ V. E. Barnes,⁽¹²⁾ F. Bedeschi,⁽¹¹⁾ S. Belforte,⁽¹¹⁾ G. Bellettini,⁽¹¹⁾ J. Bellinger,⁽¹⁷⁾
J. Bensinger,⁽²⁾ A. Beretvas,⁽¹⁴⁾ P. Berge,⁽⁴⁾ S. Bertolucci,⁽⁵⁾ S. Bhadra,⁽⁷⁾ M. Binkley,⁽⁴⁾ R. Blair,⁽¹⁾
C. Blocker,⁽²⁾ J. Boffill,⁽⁴⁾ A. W. Booth,⁽⁴⁾ G. Brandenburg,⁽⁶⁾ D. Brown,⁽⁶⁾ A. Byon,⁽¹²⁾ K. L. Byrum,⁽¹⁷⁾
M. Campbell,⁽³⁾ R. Carey,⁽⁶⁾ W. Carithers,⁽⁹⁾ D. Carlsmith,⁽¹⁷⁾ J. T. Carroll,⁽⁴⁾ R. Cashmore,⁽⁴⁾
F. Cervelli,⁽¹¹⁾ K. Chadwick,^(4,12) T. Chapin,⁽¹³⁾ G. Chiarelli,⁽¹¹⁾ W. Chinowsky,⁽⁹⁾ S. Cihangir,⁽¹⁵⁾
D. Cline,⁽¹⁷⁾ D. Connor,⁽¹⁰⁾ M. Contreras,⁽²⁾ J. Cooper,⁽⁴⁾ M. Cordelli,⁽⁵⁾ M. Curatolo,⁽⁵⁾ C. Day,⁽⁴⁾
R. DelFabbro,⁽¹¹⁾ M. Dell'Orso,⁽¹¹⁾ L. DeMortier,⁽²⁾ T. Devlin,⁽¹⁴⁾ D. DiBitonto,⁽¹⁵⁾ R. Diebold,⁽¹⁾
F. Dittus,⁽⁴⁾ A. DiVirgilio,⁽¹¹⁾ J. E. Elias,⁽⁴⁾ R. Ely,⁽⁹⁾ S. Errede,⁽⁷⁾ B. Esposito,⁽⁵⁾ B. Flaughner,⁽¹⁴⁾
E. Focardi,⁽¹¹⁾ G. W. Foster,⁽⁴⁾ M. Franklin,^(6,7) J. Freeman,⁽⁴⁾ H. Frisch,⁽³⁾ Y. Fukui,⁽⁸⁾ A. F. Garfinkel,⁽¹²⁾
P. Giannetti,⁽¹¹⁾ N. Giokaris,⁽¹³⁾ P. Giromini,⁽⁵⁾ L. Gladney,⁽¹⁰⁾ M. Gold,⁽⁹⁾ K. Goulianos,⁽¹³⁾
C. Grosso-Pilcher,⁽³⁾ C. Haber,⁽⁹⁾ S. R. Hahn,⁽¹⁰⁾ R. Handler,⁽¹⁷⁾ R. M. Harris,⁽⁹⁾ J. Hauser,⁽³⁾
T. Hessing,⁽¹⁵⁾ R. Hollebeek,⁽¹⁰⁾ P. Hu,⁽¹⁴⁾ B. Hubbard,⁽⁹⁾ P. Hurst,⁽⁷⁾ J. Huth,⁽⁴⁾ H. Jensen,⁽⁴⁾
R. P. Johnson,⁽⁴⁾ U. Joshi,⁽¹⁴⁾ R. W. Kadel,⁽⁴⁾ T. Kamon,⁽¹⁵⁾ S. Kanda,⁽¹⁶⁾ D. A. Kardelis,⁽⁷⁾
I. Karliner,⁽⁷⁾ E. Kearns,⁽⁶⁾ R. Kephart,⁽⁴⁾ P. Kesten,⁽²⁾ H. Keutelian,⁽⁷⁾ S. Kim,⁽¹⁶⁾ L. Kirsch,⁽²⁾
K. Kondo,⁽¹⁶⁾ U. Kruse,⁽⁷⁾ S. E. Kuhlmann,⁽¹²⁾ A. T. Laasanen,⁽¹²⁾ W. Li,⁽¹⁾ T. Liss,⁽³⁾ N. Lockyer,⁽¹⁰⁾
F. Marchetto,⁽¹⁵⁾ R. Markeloff,⁽¹⁷⁾ L. A. Markosky,⁽¹⁷⁾ P. McIntyre,⁽¹⁵⁾ A. Menzione,⁽¹¹⁾ T. Meyer,⁽¹⁵⁾
S. Mikamo,⁽⁸⁾ M. Miller,⁽¹⁰⁾ T. Mimashi,⁽¹⁶⁾ S. Miscetti,⁽⁵⁾ M. Mishina,⁽⁸⁾ S. Miyashita,⁽¹⁶⁾ N. Mondal,⁽¹⁷⁾
S. Mori,⁽¹⁶⁾ Y. Morita,⁽¹⁶⁾ A. Mukherjee,⁽⁴⁾ C. Newman-Holmes,⁽⁴⁾ L. Nodulman,⁽¹⁾ R. Paoletti,⁽¹¹⁾
A. Para,⁽⁴⁾ J. Patrick,⁽⁴⁾ T. J. Phillips,⁽⁶⁾ H. Piekarz,⁽²⁾ R. Plunkett,⁽¹³⁾ L. Pondrom,⁽¹⁷⁾ J. Proudfoot,⁽¹⁾
G. Punzi,⁽¹¹⁾ D. Quarrie,⁽⁴⁾ K. Ragan,⁽¹⁰⁾ G. Redlinger,⁽³⁾ J. Rhoades,⁽¹⁷⁾ F. Rimondi,⁽⁴⁾ L. Ristori,⁽¹¹⁾
T. Rohaly,⁽¹⁰⁾ A. Roodman,⁽³⁾ A. Sansoni,⁽⁵⁾ R. Sard,⁽⁷⁾ V. Scarpine,⁽⁷⁾ P. Schlabach,⁽⁷⁾ E. E. Schmidt,⁽⁴⁾

P. Schoessow,⁽¹⁾ M. H. Schub,⁽¹²⁾ R. Schwitters,⁽⁶⁾ A. Scribano,⁽¹¹⁾ S. Segler,⁽⁴⁾ M. Sekiguchi,⁽¹⁶⁾
P. Sestini,⁽¹¹⁾ M. Shapiro,⁽⁶⁾ M. Sheaff,⁽¹⁷⁾ M. Shibata,⁽¹⁶⁾ M. Shochet,⁽³⁾ J. Siegrist,⁽⁹⁾ P. Sinervo,⁽¹⁰⁾
J. Skarha,⁽¹⁷⁾ D. A. Smith,⁽⁷⁾ F. D. Snider,⁽³⁾ R. St. Denis,⁽⁶⁾ A. Stefanini,⁽¹¹⁾ Y. Takaiwa,⁽¹⁶⁾
K. Takikawa,⁽¹⁶⁾ S. Tarem,⁽²⁾ D. Theriot,⁽⁴⁾ A. Tollestrup,⁽⁴⁾ G. Tonelli,⁽¹¹⁾ Y. Tsay,⁽³⁾ F. Ukegawa,⁽¹⁶⁾
D. Underwood,⁽¹⁾ R. Vidal,⁽⁴⁾ R. G. Wagner,⁽¹⁾ R. L. Wagner,⁽⁴⁾ J. Walsh,⁽¹⁰⁾ T. Watts,⁽¹⁴⁾
R. Webb,⁽¹⁵⁾ T. Westhusing,⁽⁷⁾ S. White,⁽¹³⁾ A. Wicklund,⁽¹⁾ H. H. Williams,⁽¹⁰⁾ T. Yamanouchi,⁽⁴⁾
A. Yamashita,⁽¹⁶⁾ K. Yasuoka,⁽¹⁶⁾ G. P. Yeh,⁽⁴⁾
J. Yoh,⁽⁴⁾ F. Zetti,⁽¹¹⁾

⁽¹⁾ *Argonne National Laboratory, Argonne, Illinois 60439*

⁽²⁾ *Brandeis University, Waltham, Massachusetts 02254*

⁽³⁾ *University of Chicago, Chicago, Illinois 60637*

⁽⁴⁾ *Fermi National Accelerator Laboratory, Batavia, Illinois 60510*

⁽⁵⁾ *Laboratori Nazionali di Frascati, Istituto Nazionale di Fisica Nucleare, Frascati, Italy*

⁽⁶⁾ *Harvard University, Cambridge, Massachusetts 02138*

⁽⁷⁾ *University of Illinois, Urbana, Illinois 61801*

⁽⁸⁾ *National Laboratory for High Energy Physics (KEK), Tsukuba, Ibaraki 305, Japan*

⁽⁹⁾ *Lawrence Berkeley Laboratory, Berkeley, California 94720*

⁽¹⁰⁾ *University of Pennsylvania, Philadelphia, Pennsylvania 19104*

⁽¹¹⁾ *Istituto Nazionale di Fisica Nucleare, University and Scuola Normale Superiore of Pisa, Pisa,*

Italy

⁽¹²⁾ *Purdue University, West Lafayette, Indiana 47907*

⁽¹³⁾ *Rockefeller University, New York, New York 10021*

⁽¹⁴⁾ *Rutgers University, Piscataway, New Jersey 08854*

⁽¹⁵⁾ *Texas A&M University, College Station, Texas 77843*

(16) *University of Tsukuba, Tsukuba, Ibaraki 305, Japan*

(17) *University of Wisconsin, Madison, Wisconsin 53706*

(18) *Visitor*

ABSTRACT

We present measurements of the pseudo-rapidity (η) distribution of charged particles ($dN_{ch}/d\eta$) produced within $|\eta| \leq 3.5$ in proton-antiproton collisions at \sqrt{s} of 630 and 1800 GeV. We measure $dN_{ch}/d\eta$ at $\eta = 0$ to be $3.18 \pm 0.05(\text{stat}) \pm 0.10(\text{sys})$ at 630 GeV, and $3.95 \pm 0.02(\text{stat}) \pm 0.13(\text{sys})$ at 1800 GeV. Many systematic errors in the ratio of $dN_{ch}/d\eta$ at the two energies cancel, and we measure $1.26 \pm 0.01 \pm 0.04$ for the ratio of $dN_{ch}/d\eta$ at 1800 GeV to that at 630 GeV within $|\eta| \leq 3$. Comparing to lower energy data, we observe an increase faster than $\ln(s)$ in $dN_{ch}/d\eta$ at $\eta = 0$.

PACS number: 13.85.Hd

We present measurements of the pseudo-rapidity distribution of charged particles ($dN_{ch}/d\eta$, where the pseudo-rapidity $\eta = -\ln(\tan(\theta/2))$, and θ is the polar angle in the lab frame) produced within $|\eta| \leq 3.5$ in proton-antiproton collisions observed at center-of-mass energies (\sqrt{s}) equal to 630 and 1800 GeV. Measurements are made with the Collider Detector at Fermilab (CDF). Since the same detector and analysis are used at both energies, many systematic errors in the ratio of η distributions at the two energies cancel almost completely.

Although there exists at present no description of multiparticle production in low momentum transfer $\bar{p}p$ collisions in terms of the fundamental fields used to describe strong interactions, there are a number of phenomenological models which attempt to reproduce various average inclusive properties of multiparticle production[1]. The energy dependence of $dN_{ch}/d\eta$ is one test of such

models. Existing data, extending from $\sqrt{s} = 15$ GeV up to $\sqrt{s} = 900$ GeV [2,3,4] exhibit a rise in the value of $dN_{ch}/d\eta$ at $\eta = 0$ consistent with a $\ln(s)$ dependence on s .

CDF is an azimuthally symmetric, 4π detector at the Fermilab Tevatron collider. Details of CDF are described elsewhere [5]. The present analysis uses data from only two detector subsystems, the Vertex Time Projection Chamber (VTPC) [6] to provide charged particle tracking, and the Beam-Beam Counters (BBC) [7] to trigger the detector. Figure 1 shows a cross sectional view of one quadrant of the inner detector including the BBC and VTPC.

The BBC consists of two sets of scintillation counters placed along the beam axis 5.82 m on either side of the interaction region. The counters cover the η range $3.2 \lesssim |\eta| \lesssim 5.9$.

The VTPC is a set of eight time projection chambers which measure the trajectory of charged particles as they exit the beam pipe. The chambers provide nearly uniform acceptance over 2π in azimuth and about ± 3 units in η . Each chamber (called a module) surrounds the beam pipe and consists of two planes of sense wires attached to opposite ends of back-to-back drift regions. The sense wire planes are segmented azimuthally into octants and aligned perpendicular to the beam axis. Each octant has 24 parallel sense wires arranged in increasing distance from the beam axis.

Ionization deposited in the chamber drifts along the beam direction toward the nearest sense wire. By measuring the arrival time of the ionization, we determine the distance at which the particle crosses a wire layer within a given octant. We assign an azimuthal position corresponding to the center of the octant to tracks which traverse only a single module. An 11.5° rotation between adjacent modules allows 3-dimensional reconstruction of tracks which traverse more than one module.

For the data presented here, we achieve a measurement precision better than 0.07 units of η for $\eta > 3$, and better than 0.005 near $\eta = 0$. The chamber resolves track pairs which pass through the same octant if separated by at least 0.06 units of η ; tracks in different azimuthal segments are

unambiguously resolved.

Low density construction materials and a beryllium beam pipe minimize the amount of material particles traverse before entering the active volume. At $\eta = 0$, the amount of material corresponds to 0.5% radiation lengths, increasing to 7.5% at $\eta = 3.6$. Contamination from photon conversions and hadronic interactions is less than a few percent within $|\eta| < 3$ (see Fig. 2).

The detector trigger requires at least one hit in each set of BBC counters in coincidence with the beam crossing. The present analysis uses about 30,000 triggers at 1800 GeV and 9,400 triggers at 630 GeV collected during the 1987 run. Additional details of the minimum bias runs and the BBC trigger acceptance can be found in ref. [8].

Several offline software cuts eliminate beam-gas background and select $\bar{p}p$ collisions from the data sample. The selection procedure retains events which pass either of the following two tests: (1) a minimum of four tracks in the VTPC with at least one in each the forward and backward hemispheres; (2) an interaction point derived from VTPC information (requiring at least two tracks) within 16 cm of that determined from BBC time-of-flight (at least three hits in each set of BBC counters). We do not correct for events missed by the trigger or selection procedure.

Data from runs with one or more missing \bar{p} bunches allow estimation of the fraction of beam-gas interactions which pass the event selection criteria. We set upper limits of $< 0.2\%$ beam-gas background at 1800 GeV, and $< 2.0\%$ at 630 GeV. The background introduces negligible bias.

Additional event selection in the final analysis includes only those events with interaction vertices within ± 12 cm of the middle of individual VTPC modules. This cut avoids non-uniformities in the acceptance caused by gaps between modules. The final event sample contains about 21,000 events at 1800 GeV, and 2800 events at 630 GeV.

To be included in the η distribution, a track must traverse a minimum of 11 of the available 24 wire layers and pass an impact parameter cut. The impact parameter, defined as the longitudinal

distance from the event vertex to the track intercept with the beam axis, divided by the expected resolution, must be less than 10.

To obtain the final η distribution, the observed distribution must be corrected for geometric and kinematic acceptance, tracking efficiency, and charged particle background from decays and secondary interactions in the beam pipe and VTPC. The dots in Fig. 2 show the acceptance as a function of $|\eta|$ averaged over azimuth.

The VTPC operates in a 1.5 Tesla magnetic field coaxial with the beam axis, and the resulting curvature of tracks causes a loss of tracking efficiency for particles with transverse momentum (p_t) less than about 50 MeV/c. These tracks spiral entirely within the outer radius of the VTPC. Extrapolating the inclusive p_t spectrum[8] to $p_t = 0$, we find the fraction of such tracks to be $3\% \pm 2\%$ (for both 630 and 1800 GeV). We adjust the acceptance to include the effects of tracks below this low p_t cutoff.

The tracking efficiency is measured from a visual scan of about 400 events from the 1800 GeV sample. Mistakes made by the reconstruction program are corrected during scanning, and the corrected tracks subjected to the above track selection. The ratio of the number of accepted tracks before and after the scan yields the effective efficiency plotted as triangles in Fig. 2. Note that this quantity exceeds unity in regions where the reconstruction finds more tracks than the scan. The corrections are less than 5% over most of the η acceptance, while contributions to the systematic uncertainty are about 1.2% near $\eta = 0$, rising to about 11% for $\eta > 1.0$.

We estimate and subtract charged particle background from photon conversions, decays of neutral (and charged) particles, and secondary hadronic interactions in the beam pipe and VTPC. The squares plotted in Fig. 2 show, as a function of $|\eta|$, the fraction of tracks which contribute to the observed η distribution resulting from photon conversions. The points are calculated from Monte Carlo assuming the average photon η distribution is approximately equal to that of charged

particles [9]. Although the background level is extremely small in the central region, it rises to nearly 10% at $|\eta| = 3.5$. The plot is valid for both 630 and 1800 GeV data.

The decay of neutral kaons to charged pions is the dominant source of background from particle decays. Assuming a K/π ratio equal to 0.11 ± 0.01 at 1800 GeV [10], and 0.10 ± 0.01 at 630 GeV (extrapolating from ref. [11]), Monte Carlo studies indicate background levels between $2\text{--}3\% \pm 1\%$ over our η range. Assuming 80% of charged particles are pions, and a charged to neutral pion ratio equal to 2, we estimate Dalitz decays of neutral pions to contribute an additional 1% at all η values. All other decays (excluding contributions from charged-mode decays of η mesons [12]) contribute negligibly to the observed $dN_{ch}/d\eta$ distribution. Monte Carlo calculations indicate that background from secondary hadronic interactions is insignificant.

Corrected η distributions for both 630 GeV and 1800 GeV are plotted in Fig. 3(a). Statistical uncertainties lie entirely within the plotted symbols, while systematic uncertainties (σ for 1800 GeV) are indicated along the lower edge of the plot. Uncertainties in the tracking efficiency dominate the systematic uncertainty, and are common to both distributions. For comparison, a measurement from the CERN SPS collider performed by UA5 at $\sqrt{s} = 546$ GeV [4] is also plotted in Fig. 3(a).

From a study of the energy dependence of our corrections, we find that systematic effects in the ratio of $dN_{ch}/d\eta$ at the two energies cancel at the level of $\pm 3\%$. The ratio is plotted as a function of $|\eta|$ in Fig. 3(b). The scatter in the points is well within the systematic uncertainty, and the ratio is consistent with being flat. We obtain the value $1.26 \pm 0.01 \pm 0.04$ for the average ratio within $|\eta| \leq 3$.

Finally, for $dN_{ch}/d\eta$ at $\eta = 0$, we measure $3.18 \pm 0.05(\text{stat}) \pm 0.10(\text{sys})$ at 630 GeV, and $3.95 \pm 0.02(\text{stat}) \pm 0.13(\text{sys})$ at 1800 GeV. Figure 4 summarizes the energy dependence of $dN_{ch}/d\eta$ at $\eta = 0$ for our data and for non-single diffractive data [4,9] at lower energies. Statistical and systematic uncertainties are added linearly for the CDF points. The curves show fits to a linear dependence

on $\ln(s)$ (dashed line) and a quadratic dependence on $\ln(s)$ (solid curve). The result of the $\ln(s)$ fit is $(0.27 \pm 0.02)\ln(s) - (0.32 \pm 0.22)$, with $\chi^2 = 8.95$ for four degrees of freedom; the quadratic fit yields $(0.023 \pm 0.008)\ln^2(s) - (0.25 \pm 0.18)\ln(s) + (2.5 \pm 1.0)$ with $\chi^2 = 0.72$ for three degrees of freedom. The fits clearly favor an energy dependence stronger than $\ln(s)$, confirming the trend observed by UA5.

The CDF collaboration thanks the CDF technical support staff, and the staff of the Tevatron Collider, whose hard and successful work made this experiment possible. We also thank the staff of the Fermilab Film Analysis Lab for their invaluable assistance in the analysis. This work was supported by: the U.S. Department of Energy; the U.S. National Science Foundation; the Istituto Nazionale di Fisica Nucleare, Italy; the Ministry of Science, Culture, and Education of Japan; and the A.P. Sloan Foundation.

References

[1] see, for example:

A. Capella and J. Tran Thanh Van, *Phys. Lett.* **114B**, 450 (1982);

T.T. Chou and C.N. Yang, *Phys. Rev.* **D32**, 1692 (1985).

[2] J. Whitmore et al., *Phys. Rep.* **10C**, 273 (1974);

W.M. Morse et al., *Phys. Rev.* **D15**, 66 (1977);

C.P. Ward et al., *Nucl. Phys.* **B153**, 299 (1979).

[3] W. Thome et al., *Nucl. Phys.* **B129**, 365 (1977);

T. Akesson et al., *Phys. Lett.* **108B**, 58 (1982).

[4] G.J. Alner et al., *Z. Phys.* **C33**, 1 (1986).

[5] F. Abe et al., *Nucl. Inst. and Meth.* **A271**, 387 (1988).

- [6] F. Snider et al., Nucl. Inst. and Meth. **A268**, 75 (1988).
- [7] D. Amidei et al., Nucl. Inst. and Meth. **A269**, 51 (1988).
- [8] F. Abe et al., Phys. Rev. Lett. **61**, 1819 (1988).
- [9] K. Alpgard et al., Phys. Lett. **115B**, 71 (1982);
G.J. Alner et al., Phys. Rep. **154**, 247 (1987).
- [10] F. Abe et al., Fermi National Accelerator Laboratory, Pub-89/178-E.
- [11] G.J. Alner et al., Nucl. Phys. **B258**, 505 (1988).
- [12] CDF has not yet measured inclusive η meson production. Since no other measurements of the η/π ratio at \sqrt{s} energies comparable to those at CDF are available, we omit this correction. However, UA5 notes an excess of photons over that expected from π^0 decay alone, and quotes an upper limit of $\eta/\pi^0 = 0.30$ assuming the excess to come from η decays [9]. Under this assumption, we estimate that at most 5% of the observed $dN_{ch}/d\eta$ distribution at CDF originates from the decay of η mesons to charged particles.

Figure captions

Figure 1: Cross sectional view of one quadrant of the VTPC and BBC. Note the difference in horizontal and vertical scales.

Figure 2: Effective tracking efficiency, acceptance, and fraction of observed tracks attributed to background from photon conversions versus $|\eta|$. Curves are drawn to guide the eye.

Figure 3: (a) $dN_{ch}/d\eta$ measured by CDF at 1800 and 630 GeV, and by UA5 at 546 GeV. (b) The ratio of $dN_{ch}/d\eta$ at 1800 GeV to that at 630 GeV.

Figure 4: $dN_{ch}/d\eta$ at $\eta = 0$ as a function of \sqrt{s} measured by UA5 [4,9] and CDF. The curves are the result of fits.

Figure 1

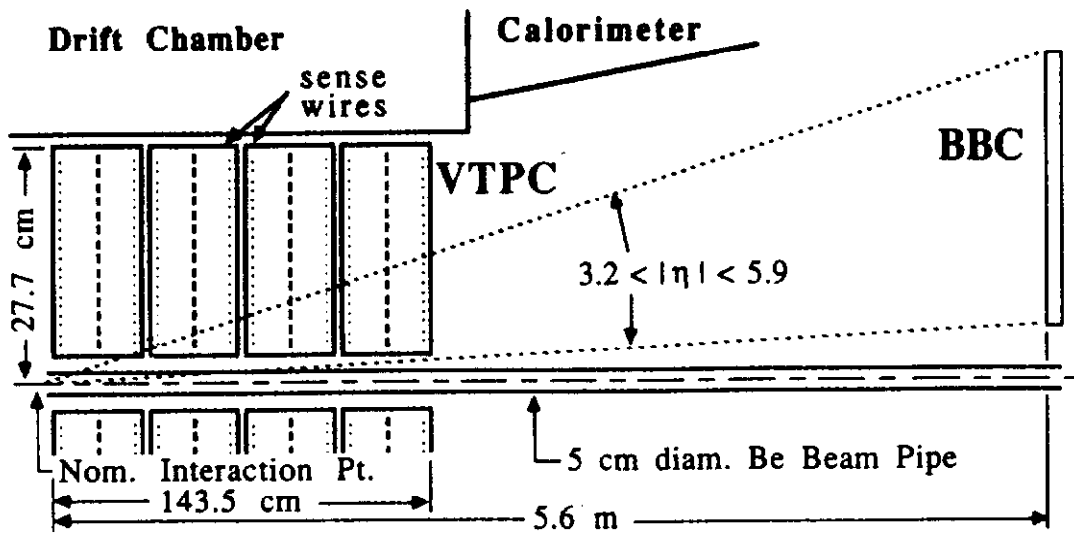


Figure 2

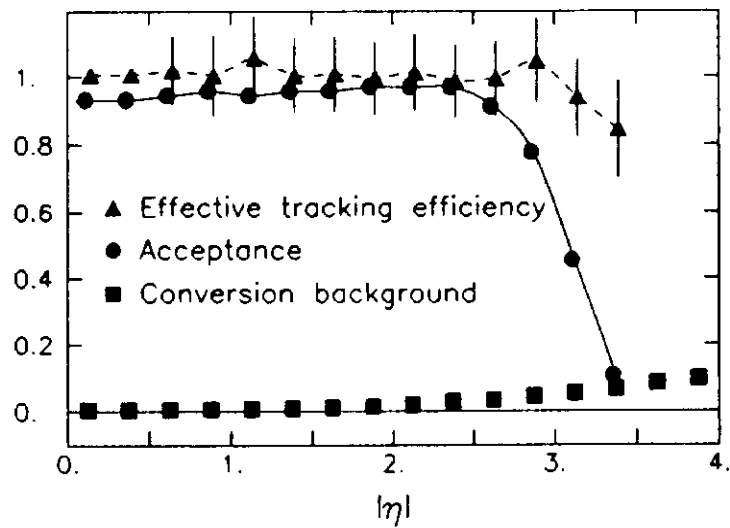


Figure 3

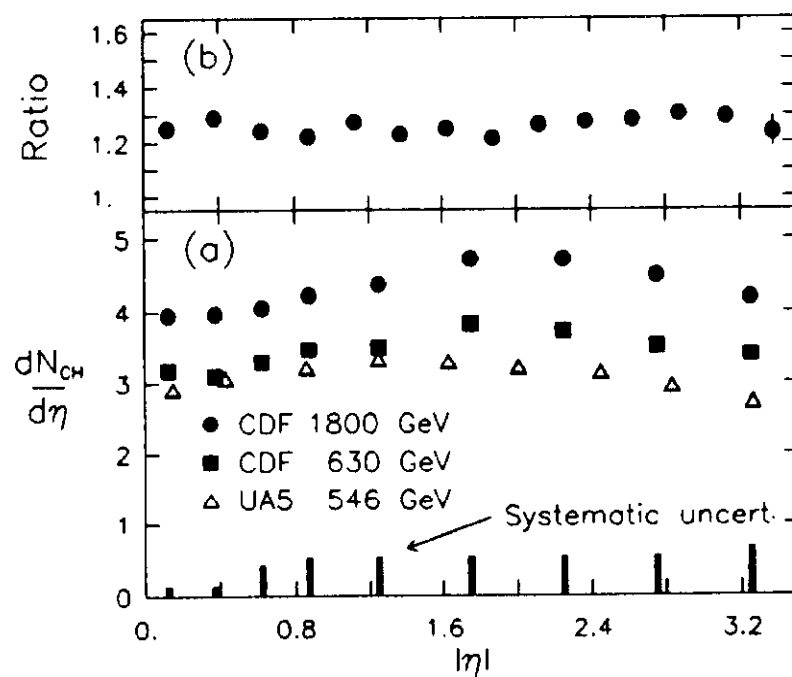


Figure 4

